Underlying simplicity of atomic population variations induced by a stochastic phase-fluctuating field

R. P. Frueholz and J. C. Camparo
Mail Stop M2-253, Electronics Technology Center, The Aerospace Corporation, P.O. Box 92957, Los Angeles, California 90009
(Received 1 March 1996)

We have examined the temporal evolution of a two-level atom in response to stochastic phase-fluctuating fields by applying perturbation theory to the optical Bloch equations written in the instantaneous frame. Our results show that the general nature of the atomic population variations is relatively simple, being composed of adiabatic and nonadiabatic components. The adiabatic response results from Fourier components of the phase variation below the system's Rabi frequency and is proportional to the product of the relatively slow phase variation and its first derivative. The nonadiabatic response has its maximum amplitude at the system's Rabi frequency, for which the atom behaves like a simple harmonic oscillator whose resonance frequency is the Rabi frequency. In this sense the atom acts as a tunable narrow-band filter. [S1050-2947(96)01710-6]

PACS number(s): 42.50.Md, 42.50.Ar, 32.80.−t

I. INTRODUCTION

One of the principle differences between optical and radiofrequency spectroscopy concerns the role of field fluctuations. Generally, the radiofrequency fields produced by quartz crystal oscillators have relative linewidths (i.e., $\Delta\nu/\nu_0$) of 10^{-11}–10^{-12} [1], while the optical fields produced by lasers have relative linewidths ranging from about 10^{-9} to 10^{-5}. As a consequence of the laser's greater (relative) stochasticity, optical analogs of radio-frequency experiments have led to different phenomena in the regime of strong-field–atom interactions. For example, Hamilton *et al.* [2] have shown that the asymmetry of the Autler-Townes doublet can be reversed, depending on the details of the laser line shape, and Lecompte *et al.* [3] and Lompre *et al.* [4] have demonstrated that multiphoton transitions excited by nonmonochromatic laser fields can exhibit enhanced excitation rates and ac Stark shifts, respectively, compared to monochromatic fields.

To date, most experimental and theoretical investigations of a stochastic field interacting with an atom have confined their attention to the *average* behavior of resonant phenomena. In contrast, our current investigations focus upon the *temporal evolution* of an atomic system in response to a stochastic field. In a previous work [5] we found that for a certain class of fluctuating field the temporal evolution of atomic density matrix elements was always quite easily interpreted when viewed in the instantaneous frame (i.e., a reference frame whose xy orientation in Bloch-vector space is determined by the field's phase). Specifically, for (phase) fluctuating fields with constant amplitude that are resonant and adiabatic (i.e., the atomic Rabi frequency is higher than any Fourier frequency comprising the phase modulation process), the Bloch-vector Z component is nearly proportional to the product of the field's fluctuating phase and the phase's first derivative, while the Y component in the instantaneous frame is approximately proportional to the fluctuating phase itself. Consequently, the temporal evolution of the Z and Y Bloch-vector components in the instantaneous frame trace out a ''figure-eight-like'' pattern. Essentially, for this class of field much of the problem's stochastic nature may be couched in terms of a sequence of stochastic orthogonal transformations in Bloch space, simplifying to a large extent the underlying atomic dynamics. In this paper we will refer to a field with constant amplitude and stochastic phase variations (characterized by a power-law dependence as the Fourier frequency of the phase variations increases) as a ''phase diffusionlike'' field and for ease of notation use the acronym PDF when referring to these fields. Our previous work dealt with ''adiabatic'' PDFs in which the great majority of the Fourier components of the stochastic phase variation are less than the system Rabi frequency.

A somewhat broader class of PDFs may be defined (i.e., ''nonadiabatic'' PDFs), where Fourier components associated with the phase modulation process are larger than the Rabi frequency Ω. For this broader class of field, the Bloch-vector evolution in the instantaneous frame displays oscillations, the frequency of which may be well above the major Fourier components associated with the phase modulation process. Here we continue our previous studies by examining the response of a two-level atom to this broader class of PDF. We will show that the oscillations in the density matrix elements are manifestations of the atom's nonadiabatic response to the PDF and are defined by the Rabi frequency. Moreover, depending upon how rapidly the fluctuating phase's Fourier components fall off with increasing Fourier frequency, we will show that the atomic temporal evolution may be dominated by either the adiabatic (i.e., figure-eight) or nonadiabatic (oscillation) atomic response to the field in the instantaneous frame.

II. COMPUTATION

The system under investigation is that of a two-level atom subjected to a resonant field that has a stochastically varying phase. The Bloch equations used to describe the system are the same as in Ref. [5], where $X^{\rm rot}$, $Y^{\rm rot}$, and Z are the coordinates of the Bloch vector in the (standard) rotating coordinate frame [6]

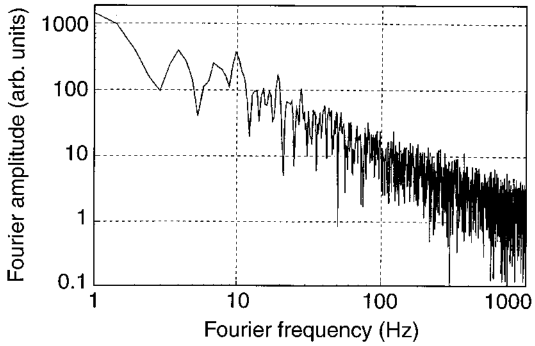

FIG. 1. Fourier transform of the phase fluctuations generated by a stochastic process in which the exponent n of Eq. (3) is set equal to unity.

$$\frac{dX^{\text{rot}}}{dt}=-\gamma X^{\text{rot}}-\Omega\ \cos[\theta(t)]Z, \tag{1a}$$

$$\frac{dY^{\text{rot}}}{dt}=-\gamma Y^{\text{rot}}-\Omega\ \sin[\theta(t)]Z, \tag{1b}$$

$$\frac{dZ}{dt}=-\gamma(Z-Z_{\text{NF}})+\Omega\ \cos[\theta(t)]X^{\text{rot}}+\Omega\ \sin[\theta(t)]Y^{\text{rot}}. \tag{1c}$$

Here we have equated the transverse and longitudinal relaxation rates ($\gamma_1=\gamma_2=\gamma$); Z_{NF} is the Z value in the absence of the resonant field, and the field's instantaneous phase fluctuation is $\theta(t)$. The stochastic phase fluctuations are broadband about a ''central'' phase modulation frequency f_c and are generated by writing the phase fluctuation in terms of two uncorrelated stochastic phase components $\varphi_{1,2}$,

$$\theta(t)=\varphi_1(t)\cos[2\pi f_c t]+\varphi_2(t)\sin[2\pi f_c t]. \tag{2}$$

The stochastic phase components are characterized by $\langle\varphi_i(t)\varphi_j(t-\tau)\rangle=\delta_{ij}R(\tau)$ and are produced by passing unit variance, Gaussian white noise through a digital filter.

The filter transfer function is

$$\widetilde{H}_n(f)=\frac{\kappa_n\sigma\alpha^{n-0.5}}{(2\pi if+\alpha)^n}, \tag{3}$$

where f is the Fourier frequency of the phase variations, κ_n is a numerical factor, σ is the standard deviation of phase fluctuations, and α is a bandwidth parameter. It is to be noted that f_c and α may be used to adjust the relative contributions of low- and high-frequency Fourier components to the overall phase modulation process $\theta(t)$. The rate of decrease in the Fourier amplitudes as f increases is determined by the value of n, and in this work we confine our attention to $n=1$, 2, and 3 ($\kappa_1=\sqrt{2}$, $\kappa_2=2$, and $\kappa_3=4/\sqrt{3}$). The digital filter is implemented using the procedure of Camparo and Lambropoulos [7], and as an example we show in Fig. 1 the Fourier transform of $\theta(t)$ for the case $n=1$, $f_c=1$ Hz, and $\alpha=10\ \text{s}^{-1}$. (In all cases to be reported here $\sigma\sim\pm1$ rad.) We note that for $n=1$ (and $f_c=0$) the stochastic process yields

$$S_{\dot\theta}(f)=4\pi^2f^2S_\theta(f)=4\pi^2f^2|\widetilde{H}_1(f)|^2=\frac{8\pi^2f^2\sigma^2\alpha}{(\alpha^2+4\pi^2f^2)}, \tag{4}$$

for which the field's frequency fluctuations are white in the limit $f\gg\alpha$, and in this limit it is similar to the traditional PDF.

The Bloch equations were solved using a fourth-order Runge-Kutta algorithm with adaptive step size and in all cases the step size was controlled by requiring the relative error in the computation of any Bloch-vector component to be less than 10^{-12}. The initial conditions for the Bloch-vector components were always $X^{\text{rot}}(0)=Y^{\text{rot}}(0)=0$ and $Z(0)=1=Z_{\text{NF}}$ with $\gamma=0.5\ \text{s}^{-1}$. As our primary interest is in relatively strong fields, the Rabi frequency was always greater than f_c. Thus the atom was exposed to (stochastic) Fourier frequency components of the phase modulation process to which it could respond both adiabatically and nonadiabatically. As noted above, the Bloch vector's temporal evolution is most simply viewed in the instantaneous frame, where the X^{inst} axis is taken along the direction of the effective field in the standard rotating frame (i.e., $\hat{\mathbf{x}}_{\text{inst}}\cdot\hat{\mathbf{x}}_{\text{rot}}=\cos[\theta(t)]$, where $\hat{\mathbf{x}}_{\text{inst}}$ and $\hat{\mathbf{x}}_{\text{rot}}$ are unit vectors in the direction of the instantaneous and rotating frame X axes, respectively). For the case of a resonant field the rotating and instantaneous frames are related by a simple time-dependent rotation in the Bloch-space xy plane. Of particular note is the fact that the Z component of the Bloch vector is unaffected by this rotation and is the same in the instantaneous, rotating, and laboratory frames.

III. RESULTS

Figure 2 shows the atomic response to two typical stochastic phase modulation patterns as a function of Rabi frequency. In both cases $2\pi f_c=10\ \text{s}^{-1}$ and the Bloch-vector trajectories for Rabi frequencies of 50, 200, and 500 s^{-1} are presented. In Figs. 2(a)–2(c) $n=1$ and $\alpha=2\times10^{-4}\ \text{s}^{-1}$, while in Figs. 2(d)–2(f) $n=3$ and $\alpha=10\ \text{s}^{-1}$. (These parameters were selected to clearly display the differing changes in atomic dynamics as the Rabi frequency is varied.) For both processes the characteristic figure-eight adiabatic response is observed along with high-frequency oscillations. The relative strength of the two contributions to the total response clearly depends upon the Rabi frequency. However, the dependence of the atomic response on Rabi frequency is completely different for the two stochastic processes. With $n=1$, the adiabatic response is observed at low Rabi frequencies, but is overwhelmed by the high-frequency oscillation at high Rabi frequencies (i.e., the adiabatic dominant response changes to the nonadiabatic dominant response as Ω increases). In contrast, when $n=3$ the adiabatic response is not apparent at low Rabi frequencies, yet as the Rabi frequency is raised the adiabatic pattern eventually becomes dominant (i.e., the nonadiabatic dominant response changes to the adiabatic dominant response as Ω increases). The general asymptotic behaviors at large Ω are valid for the indicated exponent values n regardless of the values of f_c and α (so long as $f_c<\Omega$). For the case of $n=2$, there is no clear demarcation between adiabatic and nonadiabatic evolution with Rabi frequency, though the relative contributions of the adiabatic and

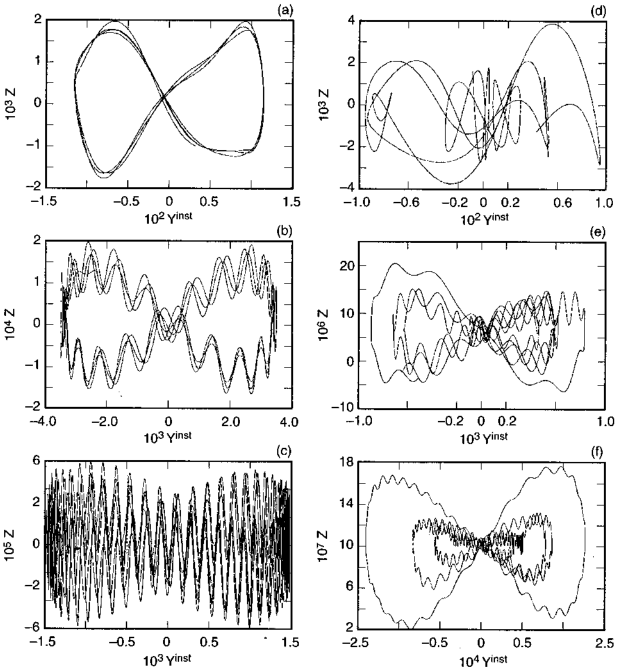

FIG. 2. Instantaneous frame Bloch-vector trajectories resulting from noise processes of Eq. (3) with (a)–(c) $n=1$ and (d)–(f) $n=3$. Rabi frequencies equal (a) and (d) 50 s^{-1}, (b) and (e) 200 s^{-1}, and (c) and (f) 500 s^{-1}. Note the different appearances of the adiabatic, figure-eight pattern as the Rabi frequency is varied for the two noise processes.

nonadiabatic response can be changed by varying the values of f_c and α.

From an intuitive perspective the reported behavior is somewhat surprising. As the Rabi frequency is increased the atomic system becomes adiabatic with respect to more and more of the Fourier frequency components of the phase variation. Consequently, one might expect that in all cases the adiabatic contribution would dominate at high Rabi frequencies as shown in Figs. 2(d)–2(f). Of course, from Figs. 2(a)–2(c) we know that this is not the case. The key observation to be made from these examples, then, is that the dynamic response of the two-level atom to PDFs depends, to a large extent, on the shape of the phase fluctuations' spectral profile [i.e., the high Fourier frequency dependence of $S_\theta(f)$].

In proceeding to understand the observed behavior, we deal with the Bloch equations in the instantaneous frame [5]. As all Bloch-vector components are taken as being in that frame, specific indications of the frame (e.g., X^{inst}) will be deleted. The relevant equations are

$$\frac{dX}{dt}=-\gamma X+\frac{d\theta}{dt}Y-\Omega Z, \tag{5a}$$

$$\frac{dY}{dt}=-\gamma Y-\frac{d\theta}{dt}X, \tag{5b}$$

$$\frac{dZ}{dt}=-\gamma(Z-Z_{\mathrm{NF}})+\Omega X. \tag{5c}$$

To mimic the stochastic nature of the phase fluctuations in a simple manner we write the phase as a sum of uncorrelated Fourier components [8]

$$\theta(t)=\theta_{\mathrm{adia}}(t)+\varepsilon\sum a_i\sin[2\pi f_i t+\psi_i]. \tag{6}$$

Here $\theta_{\mathrm{adia}}(t)$ corresponds to all Fourier components with frequencies less than the Rabi frequency, i.e., those expected to induce an adiabatic atomic response. The summation on the right-hand side of Eq. (6) is over Fourier frequencies f_i in the vicinity of the Rabi frequency and higher. The ψ_i are random and uniformly distributed between 0 and 2π, while the a_i are chosen in a manner consistent with the spectral profile of the noise process to be modeled. The parameter ε is the mean amplitude of the Fourier components near the Rabi frequency and as such $\varepsilon\sim\sqrt{\langle\theta_{\mathrm{adia}}^2\rangle}/\Omega^n$. As εa_i will typically be much less than the root-mean-square value of θ_{adia}, application of a perturbative approach to the solution to Eqs. (5) with the phase variations supplied by Eq. (6) is justified.

Each Bloch-vector component is written in the form

$$C(t)=C^{(0)}(t)+\varepsilon C^{(1)}(t), \tag{7}$$

with the superscripts on the Bloch-vector components indicating the order of the perturbation expansion to which they are related. The specific expressions for each component are substituted into Eqs. (5) along with the phase modulation given by Eq. (6). Collection of zeroth-order terms in ε produces a set of equations for $X^{(0)}$, $Y^{(0)}$, and $Z^{(0)}$ identical in form to Eqs. (5) with $\theta(t)$ replaced by $\theta(t)_{\mathrm{adia}}$. These are the same equations as analyzed in Ref. [5] and the results of that analysis for the adiabatic component of the atomic response are applicable in our current study. The first-order equations describe primarily the nonadiabatic aspects of the atomic response

$$\frac{dX^{(1)}}{dt}=-\gamma X^{(1)}+\frac{d\theta_{\mathrm{adia}}}{dt}Y^{(1)}+\left[\sum 2\pi a_i f_i\cos(2\pi f_i t+\psi_i)\right]Y^{(0)}-\Omega Z^{(1)}, \tag{8a}$$

$$\frac{dY^{(1)}}{dt}=-\gamma Y^{(1)}-\frac{d\theta_{\mathrm{adia}}}{dt}X^{(1)}-\left[\sum 2\pi a_i f_i\cos(2\pi f_i t+\psi_i)\right]X^{(0)}, \tag{8b}$$

$$\frac{dZ^{(1)}}{dt}=-\gamma Z^{(1)}+\Omega X^{(1)}. \tag{8c}$$

To proceed with the analysis we make two simplifications. $\dot{\theta}_{\mathrm{adia}}$ is in essence a fluctuating field frequency associated with the phase modulation's adiabatic components and terms containing it will have magnitudes that are generally much smaller than those of the terms containing the f_i. As a result, a reasonable simplification is to drop the terms containing $\dot{\theta}_{\mathrm{adia}}$ from Eqs. (8a) and (8b). In the same vein, the terms containing γ in these equations are also small and are removed. With these simplifications we obtain the following equation to approximately describe the first-order population variations:

$$\frac{d^2Z^{(1)}}{dt^2}+\gamma\frac{dZ^{(1)}}{dt}+\Omega^2Z^{(1)}=\left[\Omega\sum 2\pi a_i f_i\cos(2\pi f_i t+\psi_i)\right]Y^{(0)}. \tag{9}$$

Clearly the nonadiabatic contribution to the population imbalance's temporal evolution resembles that of a driven, damped harmonic oscillator, hence the nonadiabatic oscillations. The degree of damping is specified by the atomic relaxation rate, in particular the longitudinal relaxation rate, while the driving function is given by the right-hand side of Eq. (9). From Ref. [5] we know that $Y^{(0)}(t)$ is proportional to $\theta(t)_{\mathrm{adia}}$. As the Fourier frequencies comprising the adiabatic phase variations are small compared to the Rabi frequency and hence the f_i, the right-hand side of Eq. (9) remains well described by a sum of sinusoidal terms with frequencies on the order of or larger than the Rabi frequency.

The resonance denominator associated with the solution of Eq. (9) in the case of a single sinusoidal driving term provides interesting insights into the behavior of the nonadiabatic component of the atomic evolution [9]. The resonance condition is satisfied when the driving frequency equals the Rabi frequency. Consequently, the nonadiabatic atomic evolution, as it appears in the dynamics of the population imbalance, should show a strong oscillatory component at the Rabi frequency. Concomitantly, variation in the Rabi frequency should result in a variation of the principal oscillatory frequency of the nonadiabatic response. Defining $Z^{(1)}(f)$ as the nonadiabatic atomic population imbalance evolution at Fourier frequency f, the form of the resonance denominator associated with a damped, driven harmonic oscillator suggests that

$$\frac{Z^{(1)}(f>\Omega)}{Z^{(1)}(\Omega)}\approx\frac{f\gamma a_f}{a_\Omega|\Omega^2-4\pi^2f^2|}, \tag{10}$$

where a_f and a_Ω are the amplitudes of the Fourier components at the resonant frequency (Ω) and a nonresonant frequency (f), respectively (with our definition of ε, $a_\Omega\sim 1$).

These expectations are clearly shown by the exact numerical results of Fig. 3. The two-level system is subjected to a phase modulation pattern described by Eq. (3) with $f_c=5.0$ Hz, $\alpha=2\times10^{-4}$ s^{-1}, and $n=3$. Figure 3(a) shows the Fourier spectrum of the stochastic phase variations. For illustrative purposes, the parameters of Eq. (3) were selected to produce a clearly defined set of frequency components at 5 Hz allowing an obvious adiabatic response to the stochastic field. If α were larger the peak at 5 Hz would be broader and less obvious, reducing the clarity of the atomic response's adiabatic component. The Fourier transforms of the population fluctuations [Fourier transform of $Z(t)$] for the Rabi frequency equal to 20 and 50 Hz are shown in Figs. 3(b) and 3(c), respectively. In Ref. [5] it was shown that the Z response, under adiabatic conditions, displays significant

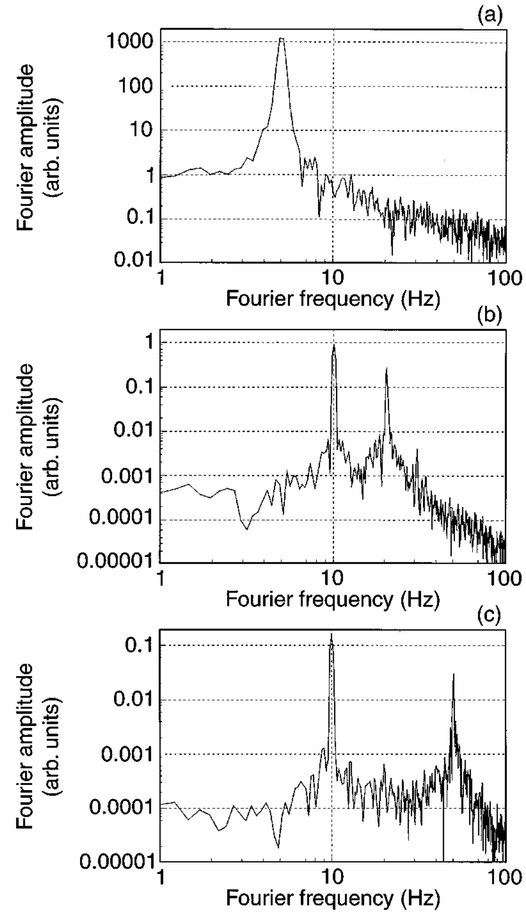

FIG. 3. (a) Fourier transform of the phase variations. Fourier transforms of atomic responses (Z component of the Bloch vector) with the Rabi frequency set to (b) $(2\pi\times20)$ s^{-1} and (c) $2\pi\times50$ s^{-1} for the noise process of Eq. (3) with $n=3$, $f_c=2\pi\times5$ s^{-1}, and $\alpha=2\times10^{-4}$ s^{-1}.

strength at twice the phase modulation frequency. In Figs. 3(b) and 3(c) the adiabatic response is, as expected, observed at $2f_c$ (i.e., 10 Hz). More importantly for the present work, however, both Figs. 3(b) and 3(c) show strong Fourier components at the Rabi frequency consistent with the resonance condition suggested by Eq. (9). As expected from Eq. (9), the nonadiabatic portion of the atomic evolution may be ''tuned'' by merely by changing the Rabi frequency. Moreover, the amplitude of the atomic response decreases more rapidly at frequencies above the Rabi frequency than at frequencies below it. This is consistent with the resonance condition for a driven, damped harmonic oscillator and the relative magnitudes of the a_i. The simple description of atomic temporal evolution in response to stochastic phase fluctuations is observed for a variety of nonadiabatic PDFs, confirming the expectation that the atomic evolution is generally the sum of an adiabatic component (tracing figure eights in the instantaneous frame) and a nonadiabatic component (Rabi frequency oscillation).

The resonance condition suggested by Eq. (9) should be distinguished from the Rabi resonance response observed by Cappeller and Mueller [10] and others [11]. In Cappeller and Mueller's investigation a two-level atom was subjected to a field with a sinusoidally varying phase, and enhanced atomic response was observed when the Rabi frequency was equal to the frequency of phase modulation. However, the resonant response was sinusoidal at *twice* the modulation frequency, similar to the current adiabatic response rather than the resonancelike, nonadiabatic response. The behavior of the two-level system in the presence of broadband excitation is clearly more complex than in the narrow-band case.

With the results of the preceding analysis it is possible to understand the apparently incongruent behavior displayed in Fig. 2. In both cases we now expect the observed patterns to be the sum of adiabatic and nonadiabatic contributions. Moreover, the relative magnitudes of the two contributions are known to be functions of the Rabi frequency and the specific noise process initiating the atomic evolution. Focusing upon the relative amplitudes of the Bloch-vector Z component, we consider first the adiabatic component. From Ref. [5] we have

$$Z^{(0)}(t) \cong \left[\frac{\gamma \Omega^2 Z_{\mathrm{NF}}}{(\gamma^2+\Omega^2)^2} \right] \theta_{\mathrm{adia}} \frac{d\theta_{\mathrm{adia}}}{dt}. \tag{11}$$

Thus, for large Rabi frequencies $Z^{(0)}(t) \sim \Omega^{-2}$. Turning to the nonadiabatic component $Z^{(1)}(t)$, we have, from Ref. [5],

$$Y^{(0)}(t) \cong \left[\frac{\gamma \Omega Z_{\mathrm{NF}}}{\gamma^2+\Omega^2} \right] \theta_{\mathrm{adia}}, \tag{12}$$

which, when used in conjunction with Eq. (9), shows that the driving term of that equation is independent of Rabi frequency in the strong-field regime. As $Z^{(1)}(t)$ is dominated by the component of the phase fluctuation process with Fourier frequency equal to the Rabi frequency,

$$|Z^{(1)}(t)| \approx a_{\Omega} Z_{\mathrm{NF}} \theta_{\mathrm{adia}}. \tag{13}$$

However, the total nonadiabatic contribution (to first order) is the product of ε and $Z^{(1)}(t)$ and ε is proportional to the Ω^{-n}. Consequently, the ratio of the atomic evolution's adiabatic component to its nonadiabatic component is proportional to Ω^{n-2}. For $n=1$, as the Rabi frequency is increased the nonadiabatic response will dominate the adiabatic response, resulting in the disappearance of the characteristic figure-eight pattern and its replacement by the unstructured pattern composed of oscillations near the Rabi frequency. This is the behavior observed in Figs. 2(a)–2(c). In contrast, if $n=3$ the adiabatic response will be dominant as the Rabi frequency is increased and the figure eight will become apparent at high Rabi frequencies. This explains the behavior of the atomic response in Figs. 2(d)–2(f). Finally, for the intermediate case in which $n=2$ the atomic response is expected to be essentially independent of the Rabi frequency, consistent with our calculations.

IV. CONCLUSIONS

In this paper we have investigated the temporal response of the two-level atom to a resonant, constant amplitude electromagnetic field that displays broadband phase noise. While the results of this study were developed by addressing three different PDFs, the conclusions are not limited to noise processes displaying their specific spectral characteristics. The finding that the atomic response may be separated into two simple adiabatic and nonadiabatic components is quite general, so long as the spectral density of phase fluctuations is reasonably "normal." That is, the phase fluctuation Fourier amplitudes at high Fourier frequencies should be smaller than those at low frequencies. Additionally, in order for the nonadiabatic atomic evolution to be dominated by oscillations at the Rabi frequency, variations in the phase fluctuation Fourier amplitudes near the Rabi frequency should not overwhelm the effect of the resonance denominator associated with the damped driven harmonic oscillator (e.g., for Fourier frequencies larger that the Rabi frequency the phase variation Fourier amplitudes should not increase more rapidly than $1/|\Omega^2 - 4\pi^2 f^2|$). In light of the noise processes typically observed experimentally, neither of these caveats is particularly restrictive.

Experimentally, it should be possible to observe the consequences of the phenomena discussed here in the population oscillations of an atomic medium. For example, since the transmitted light intensity of a weak probe through an atomic vapor is proportional to the atomic density in the absorbing quantum state, one could perform a double-resonance experiment and examine the Fourier spectrum of the weak probe's transmitted intensity variations in order to reproduce our Fig. 3. This could be realized in an optically pumped alkali-metal vapor, which has application to atomic clock technology [12]. Specifically, in Rb atomic clocks fractional population changes of several tenths of a percent are readily detected [13]. With suitable signal averaging the counter-intuitive results of Figs. 2(a)–2(c) could be manifested by examining the relative amplitude of the adiabatic and nonadiabatic components in a Fourier spectrum as a function of Rabi frequency. Moreover, the tunability of the nonadiabatic response with Rabi frequency could be demonstrated. Finally, by subjecting the atomic system to broadband noise and examining the probe's transmitted intensity variations, the atomic system's manifestation as a narrow-band filter could be demonstrated.

As a final observation, we note the utility, recognized by many authors [14], of the instantaneous frame and its value in addressing quantum-system interactions with nonmonochromatic fields. The transformation into that frame allows one to directly address the temporal variations of the field phase, a factor critical to simplifying the conceptual understanding of an atom's response to a phase varying field.

ACKNOWLEDGMENTS

The authors would like to thank B. Jaduszliwer for a critical reading of the manuscript. This work was supported under The Aerospace Corporation's Aerospace Sponsored Research Program.

[1] F. L. Walls and A. DeMarchi, IEEE Trans. Instrum. Meas. **IM-24**, 210 (1975).
[2] M. W. Hamilton, K. Arnett, S. J. Smith, D. S. Elliot, M. Dziemballa, and P. Zoller, Phys. Rev. A **36**, 178 (1987).
[3] C. Lecompte, G. Mainfray, C. Manus, and F. Sanchez, Phys. Rev. A **11**, 1009 (1975).
[4] L.-A. Lompre, G. Mainfray, C. Manus, and J. P. Marinier, J. Phys. B **14**, 4307 (1981).
[5] R. P. Frueholz and J. C. Camparo, Phys. Rev. A **52**, 472 (1995).
[6] I. I. Rabi, N. F. Ramsey, and J. Schwinger, Rev. Mod. Phys. **26**, 167 (1954).
[7] J. C. Camparo and P. Lambropoulos, Phys. Rev. A **47**, 480 (1993).
[8] See, for example, S. Goldman, *Frequency Analysis, Modulation and Noise* (McGraw-Hill, New York, 1948), Chap. 7; S. O. Rice, in *Selected Papers on Noise and Stochastic Processes*, edited by N. Wax (Dover, New York, 1954).
[9] See, for example, R. Resnick and D. Halliday, *Physics, Part I* (Wiley, New York, 1966), pp. 372–375; J. B. Vernon, *Linear Vibration Theory* (Wiley, New York, 1967).
[10] U. Cappeller and H. Mueller, Ann. Phys. (Leipzig) **42**, 250 (1985).
[11] See, for example, J. C. Camparo and R. P. Frueholz, Phys. Rev. A **38**, 6143 (1988); S. Papademetriou, S. Chakmakjian, and C. R. Stroud, Jr., J. Opt. Soc. Am. B **9**, 1182 (1992).
[12] J. C. Camparo and R. P. Frueholz, in *Proceedings of the 1993 IEEE International Frequency Control Symposium* (IEEE, Piscataway, NJ, 1993), pp. 114–119.
[13] J. C. Camparo and R. P. Frueholz, J. Appl. Phys. **59**, 301 (1986).
[14] L. Allen and J. H. Eberly, *Optical Resonance and Two-Level Atoms* (Wiley, New York, 1975), Sec. 4.6; P. Avon and C. Cohen-Tannoudji, J. Phys. B **10**, 155 (1977).